Modeling the Southern Hemisphere winter circulation using realistic zonal mean gravity wave information in the lower atmosphere

Jacobi, Ch.[+], Lilienthal, F.[+], Schmidt, T.*, de la Torre, A.[x]

[+]) *Institute for Meteorology, Universität Leipzig, Stephanstr. 3 04103 Leipzig, E-Mail: jacobi@uni-leipzig.de*
*) *Department 1: Geodesy, GFZ German Research Centre for Geosciences, Potsdam, Germany*
[x]) *Facultad de Ingeniería, Universidad Austral and CONICET, Buenos Aires, Argentina*

Summary: A mechanistic global circulation model is used to simulate the mesospheric and lower thermospheric circulation during austral winter. The model includes a gravity wave (GW) parameterization that is initiated by prescribed GW parameters in the troposphere. In standard configuration, these waves are described by a simple distribution with large amplitudes in the winter hemisphere and small ones in summer. Here we replace this distribution by a more realistic one, which is based on observations of potential GW energy using GPS radio occultations, but which is normalized to the same global mean amplitude. The model experiment shows that this new gravity wave distribution leads to weaker zonal winds in the mesosphere, a downward shift of the meridional poleward mesospheric wind jet, enhanced downwelling in the mid-to-high-latitude winter mesosphere and warming of the polar stratopause.

Zusammenfassung: Ein globales mechanistisches Zirkulationsmodell wird verwendet um die Dynamik der Mesosphäre und unteren Thermosphäre im Südwinter zu simulieren. Das Modell beinhaltet eine Schwerewellenparametrisierung die durch eine vorgeschriebene Schwerewellenverteilung in der oberen Troposphäre angetrieben wird. In der Standardkonfiguration besteht diese aus einer einfachen zonal gemittelten Verteilung mit größeren Amplituden im Winter als im Sommer. Wir ersetzen diese Verteilung durch eine realistischere, die auf der beobachteten globalen Verteilung der potentiellen Energie von Schwerewellen basiert und auf die gleiche global gemittelte Amplitude normiert wird. Das Modellexperiment zeigt, dass die neue Schwerewellenverteilung zu schwächeren zonalen Winden in der Mesosphäre, einer Verschiebung des meridionalen Jets nach unten, verstärkten Abwinden in der Mesosphäre mittlerer und höherer Breiten im Winter, und einer Erwärmung der polaren Winterstratopause führt.

1. Introduction

The dynamics of the mesosphere and lower thermosphere (MLT) are determined by the mesospheric zonal jets and the influence of gravity waves (GWs). GWs are mainly forced in the troposphere, the major sources being orography and convection. Propagating upward, they may encounter critical lines or break selectively depending on their intrinsic phase speed so that waves with phase speeds close to the background wind may only propagate if their amplitudes are small. Thus, in the upper mesosphere mainly GWs with phase speeds in the opposite direction of the mean flow are remaining. If these break they deposit momentum on the mean flow in opposite direction of the latter, leading to the observed MLT wind reversal.

GWs have horizontal wavelengths of tens to hundreds of km. Therefore they are at least partly of subgrid scale in global circulation models. This means that the waves have to be parameterized and also their sources have to be described adequately. Climate or weather-forecasting models traditionally parameterize GW sources in the troposphere especially by mountain-wave parameterizations e.g. to improve i.e. tropospheric wind jets (Alexander et al. 2010; Geller et al., 2013). Models for the middle atmosphere, however, focus on parameterizations not necessarily driven by source parameterization with regard to stratospheric and mesospheric dynamics. Initializing GW can be done by introducing some prescribed GW distribution in the lower atmosphere. In mechanistic models that are primarily used for sensitivity experiments, this distribution may be described by a simple function. Alternatively, one may describe the GW source distribution based on observed GW fields.

Such observed fields can be obtained from radio occultation (RO) measurements based on radio links between a GPS satellite and a low-earth orbiting (LEO) satellite (Kursinski et al., 1997). Since GPS ROs deliver temperature profiles in the upper troposphere and lower stratosphere, temperature fluctuations can be obtained by removing the background either through vertical or horizontal detrending (e.g. Tsuda et al., 2000; Ern et al., 2011; Schmidt et al., 2016). Then, potential energy E_p can be obtained from the temperature fluctuations, which is one measure for GW activity. The first climatology of GPS RO E_p has been presented by Tsuda et al. (2000) using GPS-MET satellite observations, but starting with CHAMP a much larger data base is available (e.g. Ratnam et al., 2004; de la Torre et al., 2006) and high-resolution observations from the 6-satellite constellation FORMOSAT-3/COSMIC and additional datasets are available now.

In this paper, we use a zonal mean GW distribution based on GPS RO E_p as input for the GW parameterization in a mechanistic circulation model. We focus on austral winter, because the strong SH polar vortex together with characteristic GW enhancements especially over South American and Antarctic mountains leads to significant deviations of GW from a simple, horizontally isotropic distribution. This GW distribution may have significant influence also for the upper atmosphere (de la Torre at al., 2014).

2. Model description

The Middle and Upper Atmosphere Model MUAM (Pogoreltsev et al., 2007) is a 3D mechanistic model of the neutral atmospheric circulation extended from the 1000 hPa surface up to the thermosphere. It based on the Cologne Model of the Middle Atmosphere-Leipzig Institute for Meteorology (COMMA-LIM, Fröhlich et al., 2003; Jacobi et al., 2006). The MUAM is a grid-point model with horizontal (latitude/longitude) resolution of 5°×5.625°, and with up to 60 levels evenly spaced in the non-dimensional log-pressure height $x = \ln(p_s/p)$ with p as pressure, p_s = 1000 hPa as a reference pressure. The step-size is constant with $\Delta x = 0.4$, which corresponds to 2.842 km in log-pressure height $h = x \cdot H$ and H as the scale height of 7 km. The model allows using an arbitrary number of levels (ranging from 48 to 60) with the same vertical resolution. In the 56-level version used here the upper boundary is placed at $x = 22.4$ which corresponds to a log-pressure height of about 150 km and a geopotential height of about 300 km depending on the thermospheric temperature. However, in the analysis we restrict ourselves to the mesosphere and lowermost thermosphere because we are interested in the GW mean flow interaction in the mesosphere here.

The model solves the primitive equations in flux form at a time step of 225 s in the 56-level version following a Matsuno integration scheme (Matsuno, 1966). The model equations are given, e.g., by Jakobs et al. (1986). MUAM includes infrared and solar radiation parameterizations to enable the forcing of solar tides through ozone and water vapor absorption. Ozone and water vapor fields are prescribed. Because the model does not include a detailed troposphere, zonal mean reanalysis data are assimilated in the troposphere and lower stratosphere below 30 km. Stationary planetary waves also taken from reanalyses are assimilated at the lower boundary. In addition, traveling planetary waves can be forced depending on the respective scientific question.

The GW parameterization currently used in MUAM is based on the linear one by Jakobs (1986) but extended especially for multiple breaking levels (Fröhlich et al., 2003; Jacobi et al., 2006; Pogoreltsev et al., 2007). The GWs are included in the model in the upper troposphere at 10 km, and the global amplitude distribution is prescribed. This is usually realized using a simple zonal mean amplitude distribution weighted meridionally by a hyperbolic tangent and with maximum in the winter hemisphere. It is adjusted in such a way that the global mean vertical wind amplitude at the forcing level is 1 cm/s (see also Fig. 3 below). In the GW parameterization, 48 waves are initialized with six different phase speeds in eight directions.

Zonal mean monthly mean temperatures and winds simulated with a model run using the standard configuration are shown in Fig. 1. We show zonal mean background temperatures (a), zonal (b), meridional (c) and vertical winds (d), and gravity wave fluxes (e) and acceleration of the mean wind by GW (f). We note a relatively strong zonal mesospheric wind jet, compared to earlier empirical climatologies like CIRA86 (Fleming et al., 1990) or the radar based GEWM (Portnyagin et al., 2004). However, CIRA winds are gradient winds calculated from geopotential heights and therefore may deviate from observed winds in the presence of strong GW acceleration on the mean flow, and the GEWM does not include radar winds between 44°S (Christchurch) and 68°S (Mawson) and therefore cannot be used for a validation of the MUAM results at 50-60°S. However, also UARS Reference Atmosphere Project (URAP) winds

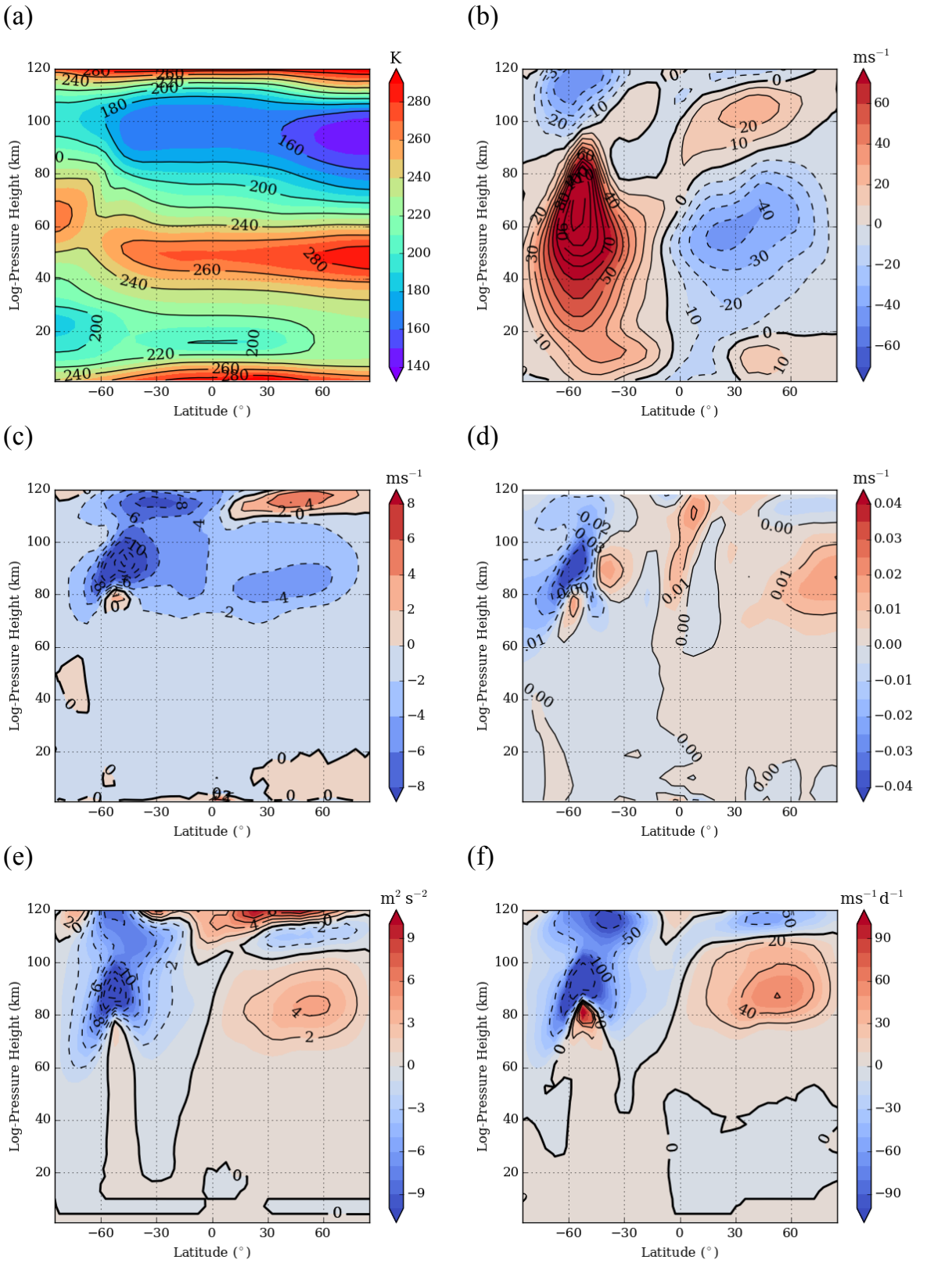

Fig. 1: Middle atmosphere (a) temperature (b) zonal wind (c) meridional wind and (d) vertical wind as simulated by MUAM for July using standard configuration of the gravity wave routine. Temperature is given in K and winds in m/s. The lower panels display (e) zonal GW flux in m^2s^{-2} and (f) zonal mean flow acceleration through GW in m/s/day. Parameters are shown as zonal means.

derived from satellite observations (Swinbank and Ortland, 2013; see also Smith, 2012) do not show such a strong maximum near 60°S, although a small zonal wind maximum is observed at the mesopause near 60°S which is partly seen in the CIRA climatology but very weak in the GEWM. The very strong wind jet up to the MLT at 50-60°S in MUAM is a consequence of the very strong, although realistic, polar night jet introduced into the model by the ERA climatology used below 30 km. This eastward jet leads to very large intrinsic phase speeds of westward traveling GW and consequently high breaking levels, so that the eastward jet in the mesosphere is decelerated only above 80 km. This also leads to a relatively high and strong poleward meridional jet in particular at higher midlatitudes. Temperatures near the mesopause in Fig 1 (a) are slightly lower than reported from satellite observations (e.g., Xu et al., 2007; Smith, 2012).

3. Austral winter long-term mean gravity waves

Instead of the zonal mean arbitrary GW fields in the standard run, we now apply a realistic, but still zonal mean GW climatology that is based on GPS RO E_p distributions. E_p is calculated using temperature profiles in the stratosphere derived from RO using FORMOSAT-3/COSMIC and MetOP satellites. The method bases on temperature anomalies in grids of 5°×10° in latitude and longitude that have been calculated after horizontal detrending, i.e. removing mean and wavenumbers 1-6 (Schmidt et al., 2016). Data from 2007-2013 with vertical steps of 100 m have been used, which have been averaged over 25-35 km altitude. E_p from the troposphere at 10 km, i.e. directly from the launch level of GW in MUAM, cannot be used because after detrending temperature residuals there are not only due to GW but also to mesoscale circulation systems. The map for July is shown in Fig. 2. One can see an enhancement of E_p near the equator that is due to convective GWs, and large E_p around 60°S, connected with the polar vortex. Further enhancement is visible east of the Andes and above all around the Antarctic Peninsula.

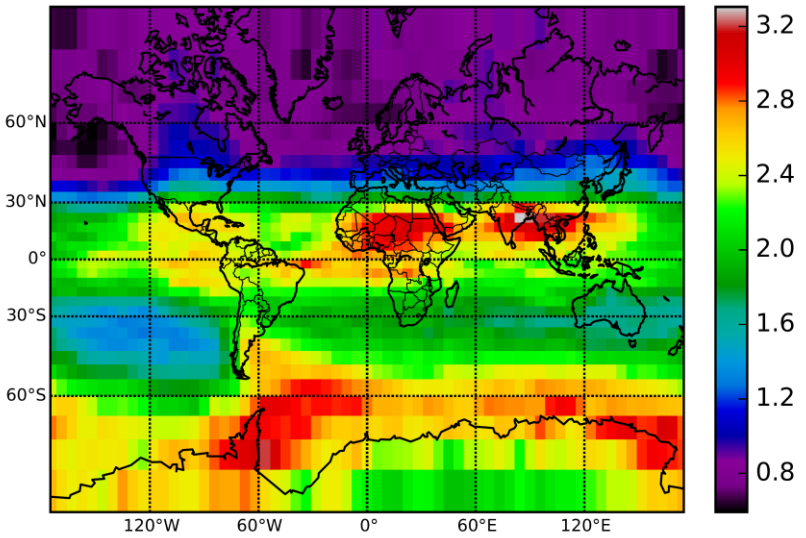

Fig. 2: Global map of 2007-2013 mean E_p (in J/kg) in July averaged between 25 and 35 km altitude.

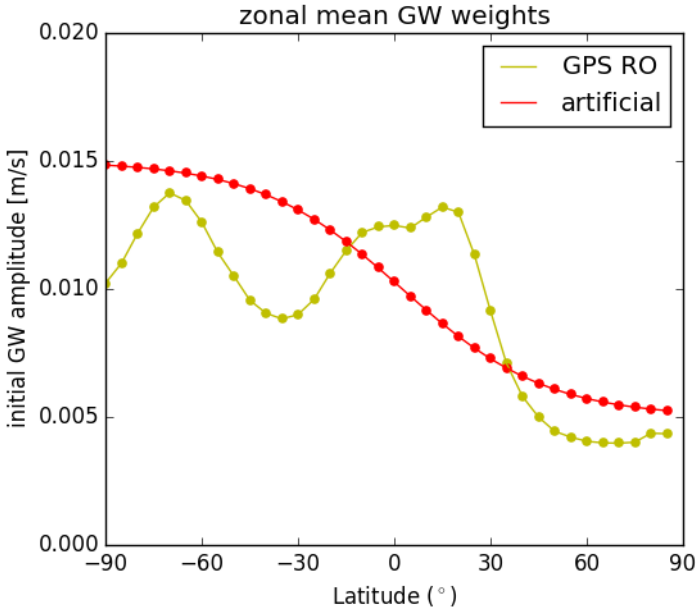

Fig. 3: GW vertical wind amplitudes for the standard run (red) and based on the GPS RO E_p distribution shown in Fig. 2.

In our model experiment we use a zonal mean GW distribution based on the long-term observations shown in Fig. 2 normalized by their E_p global average. In Fig. 3 the zonal mean vertical wind amplitudes of the launched GW are shown. The zonal mean data have been adjusted in such a way that the global mean GW amplitude again is 1 cm/s so that the results can be directly compared. One can see from Fig. 3 that between 10°S and 30°N the new amplitudes are enhanced due to the equatorial GW maximum, while for the other regions they are slightly smaller. In the Southern Hemisphere there is a modulation with a maximum at 60-70°S, which is due to GW forced by the polar vortex, the continental edge of Antarctica, and the Antarctic Peninsula.

4. MUAM results using realistic gravity wave distribution

Fig. 4 shows modeled temperatures, winds and GW fluxes and acceleration from the new run, and the differences between the new run and the reference run as isolines in the respective panels. Considering the summer hemisphere poleward of 30°N the GW acceleration (Fig. 4,f) in the upper mesosphere above 70 km is increased. This is due to the smaller amplitudes, so that GW may propagate to higher altitudes and increase the GW flux and then the GW acceleration there. At lower latitudes, GW fluxes and acceleration is increased in the stratosphere and lower mesosphere. Here the amplitudes of the new run are larger, so that the GW break earlier and at lower altitudes. This leads to a region of decreased zonal wind jet (Fig. 4,b) at its upper part (the zonal wind is negative so that positive values in Fig 4 (b) denote decreasing jet).

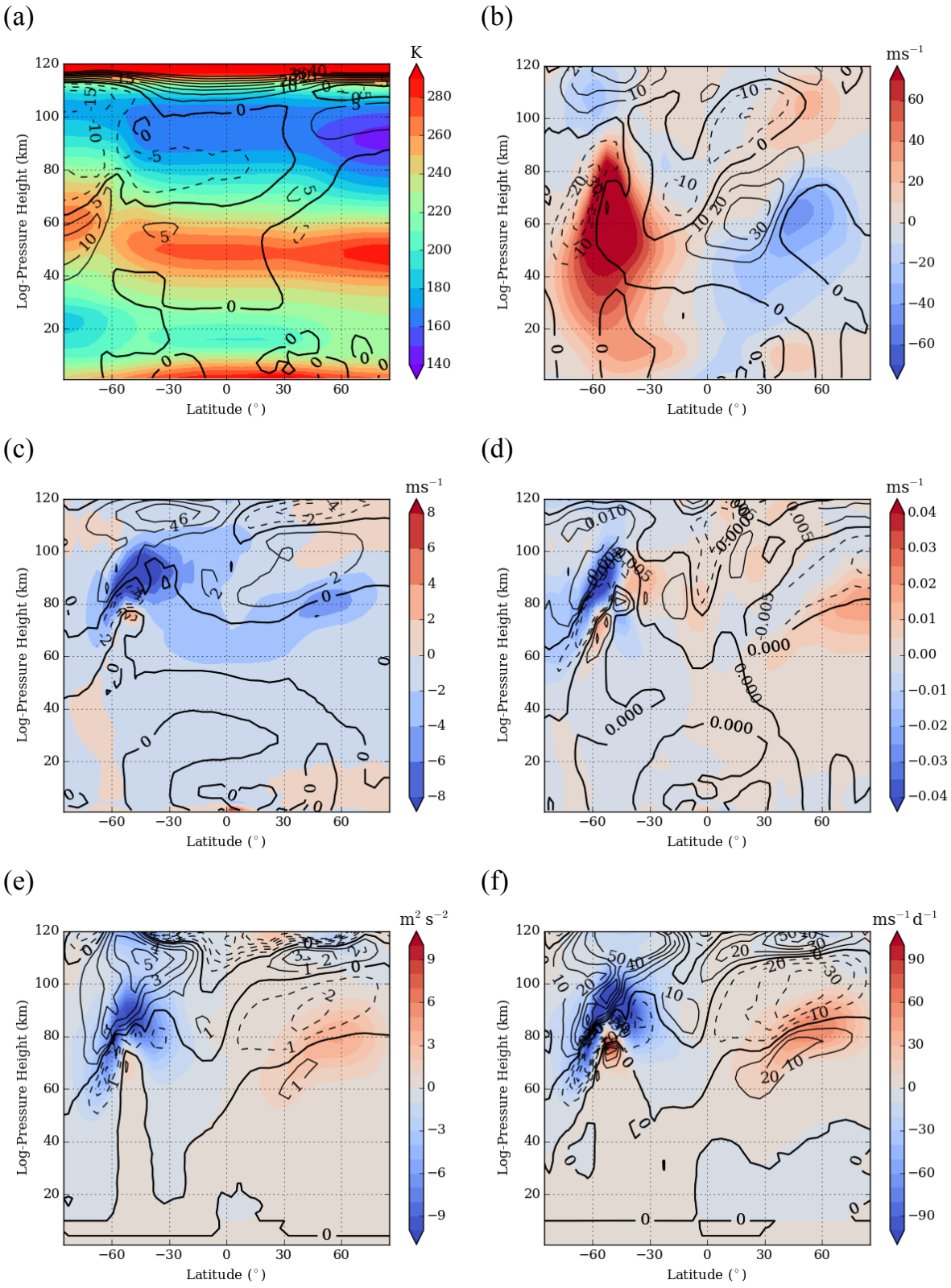

Fig. 4: Middle atmosphere (a) temperature (b) zonal wind (c) meridional wind and (d) vertical wind as simulated by MUAM for July using gravity wave amplitudes based on GPS RO potential energy. Temperature is given in K and winds in m/s. The lower panels display (e) zonal GW flux in m^2s^{-2} and (f) zonal mean flow acceleration through GW in m/s/day. The differences w.r.t. the standard run are given as contour lines.

The effects in the Southern Hemisphere are even more dramatic. The generally smaller amplitudes of GW at the launch level mean that the waves can propagate easier through the stratosphere, and the GW flux is increased in the upper mesosphere (Fig. 4,e). Note that the flux is westward and therefore negative. Then, the GW acceleration at the upper part of the westerly wind jet is increased (Fig. 4 (f)), so that the zonal wind jet is decreased in particular at its zonal flank (Fig. 4 (b)), which leads to a better correspondence with URAP winds (Smith, 2012). This is connected with stronger poleward meridional wind (Fig. 4 (c)), stronger downward winds (Fig. 4 (d)) and more warming in the polar stratosphere and lowermost mesosphere (Fig. 4 (a)). Above the region of strongest GW interaction the situation is reversed. Because the westerly wind jet is reduced the intrinsic phase speeds of the GW decrease and the propagation conditions for GW become worse, resulting in less (positive differences because of the negative fluxes) GW and finally more cooling near the mesopause, in particular slightly below it. Since MUAM underestimates mesopause temperatures, this change does not lead to a more realistic description there, and in future experiments slightly larger GW amplitudes at the launch level should be used.

5. Conclusions

In this paper we replaced the simple GW source distribution in the GW parameterization of the MUAM model by a more realistic one, which is based on observations of potential GW energy using GPS RO E_p obtained from FORMOSAT-3/COSMIC and MetOP observations. Because in the Southern Hemisphere winter the GW distribution markedly deviates from an isotropic one, we focus on austral winter here.

The model experiment shows that using this new, more realistic, source GW distribution leads to weaker zonal winds in the mesosphere, a downward shift of the meridional poleward mesospheric wind jet especially at the flanks of the mesospheric jets, and enhanced downwelling in the mid-to-high-latitude winter mesosphere. This leads to a warming of the winter polar stratopause w.r.t. the model results in standard configuration. The results show that realistic GW sources lead to a significantly modified MLT circulation and that GW distributions as an input for circulation model GW parameterizations have to be chosen carefully.

Much of the effect on the mean circulation, however, is due to the general level of GW amplitudes. In the distribution based on E_p, the zonal mean amplitudes are smaller which leads to a deceleration of the mesospheric jet and finally to a cooling of the mesopause region in particular in its lower part. Since MUAM slightly overestimates mesopause temperatures, in future experiments slightly enhanced GW amplitudes at the launch levels should be considered.

Acknowledgements

This study has been supported by BMBF under grant # 01DN14001 and by MINCyT under BID-PICT 1097.

References

Alexander, M. J., Geller, M., McLandress, C., Polavarapu, S., Preusse, P., Sassi, F., Sato, K., Eckermann, S., Ern, M., Hertzog, A., Kawatani, Y., Pulido, M., Shaw, T. A., Sigmond, M., Vincent, R., Watanabe, S., 2010: Recent developments in gravity-wave effects in climate models and the global distribution of gravity-wave momentum flux from observations and models, Q.J.R. Meteorol. Soc., 136, 1103–1124. doi: 10.1002/qj.637

de la Torre, A., Schmidt, T., Wickert, J., 2006: A global analysis of wave potential energy in the lower stratosphere derived from 5 years of GPS radio occultation data with CHAMP, Geophys. Res. Lett., 33, L24809, doi:10.1029/2006GL027696.

de la Torre, A., Alexander, P., Llamedo, P., Hierro, R., Nava, B., Radicella, S., Schmidt, T., Wickert, J., 2014: Wave activity at ionospheric heights above the Andes Mountains detected from FORMOSAT-3/COSMIC GPS radio occultation data, J. Geophys. Res. Space Physics, 119, 2046–2051, doi:10.1002/2013JA018870.

Ern, M., Preusse, P., Gille, J. C., Hepplewhite, C. L., Mlynczak, M. G., Russell III, J. M., Riese, M., 2011: Implications for atmospheric dynamics derived from global observations of gravity wave momentum flux in stratosphere and mesosphere, J. Geophys. Res., 116, D19107, doi:10.1029/2011JD015821.

Fleming, E. L., Chandra, S., Barnett, J. J., Corney, M., 1990: Zonal mean temperature, pressure, zonal wind and geopotential height as function of latitude, Adv. Space. Res, 10(12), 11-59.

Fröhlich, K., Pogoreltsev, A., Jacobi, Ch., 2003: The 48-layer COMMA-LIM model, Rep. Inst. Meteorol. Univ. Leipzig, 30, 157-185.

Geller, M. A., Alexander, M. J., Love, P. T., Bacmeister, J., Ern, M., Hertzog, A., Manzini, E., Preusse, P., Sato, K., Scaife, A. A., Zhou, T., 2013: A comparison between gravity wave momentum fluxes in observations and climate models, J. Climate, 26, 6383–6405, doi:http://dx.doi.org/10.1175/JCLI-D-12-00545.1

Jakobs, H. J., Bischof, M., Ebel, A., Speth, P., 1986: Simulation of gravity wave effects under solstice conditions using a 3-D circulation model of the middle atmosphere, J. Atmos. Terr. Phys., 48, 1203-1223, doi:10.1016/0021-9169(86)90040-1.

Kursinski, E. R., Hajj, G. A., Schofield, J. T., Linfield, R. P., Hardy, K. R., 1997: Observing Earth's atmosphere with radio occultation measurements using the Global Positioning System, J. Geophys. Res., 102, 23429–23465, doi:10.1029/97JD01569.

Matsuno, T., 1966: Numerical Integrations of primitive equations by use of a simulated backward difference method, J. Meteor. Soc. Japan, Ser. II, 44, 76-84.

Pogoreltsev, A. I., Vlasov, A. A., Fröhlich, K., Jacobi, Ch., 2007: Planetary waves in coupling the lower and upper atmosphere, J. Atmos. Sol.-Terr. Phys., 69, 2083-2101, doi: 10.1016/j.jastp.2007.05.014.

Portnyagin, Yu., T. Solovjova, T., Merzlyakov, E., Forbes, J., Palo, S., Ortland, D., Hocking, W., MacDougall, J., Thayaparan, T., Manson, A., Meek, C., Hoffmann, P., Singer, W., Mitchell, N., Pancheva, D., Igarashi, K., Murayama, Y., Jacobi, Ch., Kürschner, D., Fahrutdinova, A., Korotyshkin, D., Clark, R., Tailor, M., Franke, S., Fritts, D., Tsuda, T., Nakamura, T., Gurubaran, S., Rajaram, R., Vincent, R., Kovalam, S., Batista, P., Poole, G., Malinga, S., Fraser, G., Murphy, D., Riggin, D., Aso,

T., Tsutsumi, M., 2004: Mesosphere/lower thermosphere prevailing wind model, Adv. Space Res., 34, 1755-1762, doi:10.1016/j.asr.2003.04.058.

Ratnam, M. V., Tetzlaff, G., Jacobi, Ch., 2004: Global and seasonal variations of stratospheric gravity wave activity deduced from the CHAllenging Minisatellite Payload (CHAMP)-GPS Satellite. J. Atmos. Sci. 61, 1610-1620.

Schmidt, T., Alexander, P., de la Torre, A., 2016: Stratospheric gravity wave momentum flux from radio occultations, J. Geophys. Res. Atmos., 121, 4443–4467, doi:10.1002/2015JD024135.

Smith, A. K., 2012: Global dynamics of the MLT, Surv. Geophys., 33, 1177–1230, doi:10.1007/s10712-012-9196-9.

Swinbank, R., Ortland, D. A., 2003: Compilation of wind data for the Upper Atmosphere Research Satellite (UARS) Reference Atmosphere Project, J. Geophys. Res., 108, 4615, doi:10.1029/2002JD003135.

Tsuda, T., Nishida, M., Rocken, C., Ware, R. H., 2000:, A global morphology of gravity wave activity in the stratosphere revealed by the GPS Occultation data (GPS/MET), J. Geophys. Res., 105, 7257–7273, doi:10.1029/1999JD901005.

Xu, J., Smith, A. K., Yuan, W., Liu, H.-L., Wu, Q., Mlynczak, M. G., Russell III, J. M., 2007: Global structure and long-term variations of zonal mean temperature observed by TIMED/SABER, J. Geophys. Res., 112, D24106, doi:10.1029/2007JD008546.